

Discriminating multi-partite entangled states

Christian Schmid^{1,2}, Nikolai Kiesel^{1,2}, Wiesław Laskowski³,
Witlef Wieczorek^{1,2}, Marek Żukowski³ and Harald Weinfurter^{1,2}

¹*Department für Physik, Ludwig-Maximilians-Universität, D-80797 München, Germany*

²*Max-Planck-Institut für Quantenoptik, D-85748 Garching, Germany*

³*Instytut Fizyki Teoretycznej i Astrofizyki, Uniwersytet Gdański, PL-80-952 Gdańsk, Poland*

(Dated: November 2, 2018)

The variety of multi-partite entangled states enables numerous applications in novel quantum information tasks. In order to compare the suitability of different states from a *theoretical* point of view classifications have been introduced. Accordingly, here we derive criteria and demonstrate how to *experimentally* discriminate an observed state against the ones of certain other classes of multi-partite entangled states. Our method, originating in Bell inequalities, adds an important tool for the characterization of multi-party entanglement.

PACS numbers: 03.65.Ud, 03.67.Mn, 03.67.-a.

Entanglement is the crucial resource for quantum information processing and as such the "currency" to pay with in almost all applications. For two-partite quantum states measures have been developed that uniquely specify the value of this resource. In contrast, for n-partite states the picture changes significantly. First, one has to distinguish not only between fully separable or entangled, but also between genuine n-partite, bi-, and tri-separable entangled states, etc. Second, even states with the same level of separability are different in the sense that they have, for example, different Schmidt rank [1] or that they cannot be transformed into each other, e.g., by, local unitary (LU) or, more generally, by stochastic local operations and classical communication (SLOCC) [2, 3]. From an experimental point of view, classifying states according to the latter property is reasonable, as states from one SLOCC-class are suited for the same multi-party quantum communication applications. Thus, for the usage of multi-partite states it is of importance to know not only the *amount* but also the *type* of entanglement contained in a particular state. In other words, the value *and* the type of the "currency" is what matters.

Tools to detect the entanglement of a state exist, most prominently entanglement witnesses [4]. An alternative method, relying on the correlations between results obtained by local measurements, are Bell inequalities. Being originally devised to test fundamental issues of quantum physics they allow to distinguish entangled from separable two-qubit quantum systems [5, 6]. Bell inequalities, meanwhile extended to three- and more partite quantum states [7, 8, 9], can thus serve as witness for both entanglement and the violation of local realism. Recently it was observed that for each graph state all non-vanishing correlations (or even a restricted number thereof) form a Bell-inequality, which is maximally violated only by the respective quantum state [10, 11]. In particular, the Bell inequality for the four-qubit cluster state is not violated at all by GHZ states [10]. Naturally several questions arise: Whether one can in general apply such Bell inequalities to discriminate particular states from other classes of multi-partite entangled states, if so,

whether they can also be constructed and applied for non-graph states, and finally, whether there are other operators that allow to experimentally discriminate entanglement classes.

In this article we address these problems starting from Bell inequalities. We present a way to construct Bell operators [12] that are *characteristic* for a particular quantum state, i.e., operators that have maximal expectation value for this multi-partite state, only. With respect to experimental applications we further aim that the expectation value can be obtained by a minimal number of measurement settings. Under certain conditions, we can relax the initial requirement that characteristic operators have to be also Bell operators, which allows further reduction of the number of settings. Comparison of the experimentally obtained expectation values with the maximal expectation values for states from other entanglement classes enables us to clearly distinguish observed states from other multi-party entangled states.

In order to construct a Bell operator, we exploit the fact that certain correlations between measurement results on individual qubits are specific for multi-partite quantum states [9]. All correlations for a state $|X\rangle$ are summarized by the correlation tensor T . If we focus on the case of four qubits, then $T_{ijkl} = \langle X | (\sigma_i \otimes \sigma_j \otimes \sigma_k \otimes \sigma_l) | X \rangle$, with $i, j, k, l \in \{0, x, y, z\}$, where $\sigma_0 = \mathbf{1}$ and $\sigma_{x,y,z}$ are the Pauli spin operators. To obtain a Bell operator $\hat{\mathcal{B}}_X$ which is characteristic for a state $|X\rangle$, we require that $|X\rangle$ is the eigenstate of $\hat{\mathcal{B}}_X$ with the highest eigenvalue λ_{\max} . If the eigenstate is not degenerate, this implies that $\hat{\mathcal{B}}_X$, acting on another state cannot lead to an expectation value greater or equal λ_{\max} .

An operator, which is in general not a Bell operator, but trivially fulfills the condition to have $|X\rangle$ as the only eigenstate with $\lambda_{\max} = 1$, is the projector or fidelity operator $\hat{\mathcal{F}}_X = |X\rangle\langle X|$ and

$$\hat{\mathcal{F}}_X = \frac{1}{16} \sum_{i,j,k,l} T_{ijkl} (\sigma_i \otimes \sigma_j \otimes \sigma_k \otimes \sigma_l). \quad (1)$$

For most of the relevant quantum states the major part

of the 256 coefficients T_{ijkl} is zero. Therefore, the number of measurement settings necessary for the evaluation of $\hat{\mathcal{F}}_X$ is much smaller than for a complete state tomography. We consider the non-vanishing terms as relevant correlations for characterizing the state and take them as a starting point for the construction of $\hat{\mathcal{B}}_X$. As we will see in the following two examples, there are quantum states for which a small subset of the relevant correlations is enough to construct $\hat{\mathcal{B}}_X$. Once this is accomplished one can calculate the upper bound, v_Y^* , on the expectation values $v_Y = \langle Y | \hat{\mathcal{B}}_X | Y \rangle = \langle \hat{\mathcal{B}}_X \rangle_Y$ for states $|Y\rangle$ which belong to other classes than $|X\rangle$. Consequently, a state under investigation with $\langle \hat{\mathcal{B}}_X \rangle_Z = v_Z$ cannot be an element of any class of states with $v_Y^* < v_Z$.

Note, $\langle \hat{\mathcal{B}}_X \rangle$ induces a particular ordering of states which is neither absolute nor related to some entanglement of the states and, similarly to the entanglement witness, depends on the operator $\hat{\mathcal{B}}_X$. Yet, now we do not only detect higher or lower degree of entanglement: we distinguish different types of entanglement. One might say that a state with a higher $\langle \hat{\mathcal{B}}_X \rangle$ is more " $|X\rangle$ -type" entangled. The same is true for a mixed state ρ with expectation value $v_\rho = \text{Tr}[\hat{\mathcal{B}}_X \rho] = \langle \hat{\mathcal{B}}_X \rangle_\rho$, in the sense that it cannot solely be expressed as a mixture of pure states $|Y_i\rangle$ with $v_{Y_i}^* < v_\rho$, but it has to contain contributions with a higher " X -type" entanglement.

Summarizing, we point at the fact that one can obtain a witness of " $|X\rangle$ -type" entanglement by constructing a discrimination operator, which has $|X\rangle$ as non-degenerate eigenvector with the highest eigenvalue. After all, such an operator is not unique, neither does it necessarily have to be a Bell operator. However, a Bell operator unconditionally detects the entanglement of the investigated state, even if the state space is not fully known. For example, witness operators might detect a state to be entangled though a description of measurement results based on local realistic models, or for that purpose, based on separable states in higher dimensional Hilbert spaces, is possible [13]. If one trusts in the representation of the state, as shown below, even more efficient operators for state discrimination can be devised.

Let us now apply our method to the state $|\Psi_4\rangle$ [14]:

$$|\Psi_4\rangle = \frac{1}{\sqrt{3}}(|0011\rangle + |1100\rangle - \frac{1}{2}(|0101\rangle + |0110\rangle + |1001\rangle + |1010\rangle)). \quad (2)$$

This state was observed in multi-photon experiments [15] and can be used, for example, for decoherence free quantum communication [16], quantum telecloning [17], and multi-party secret sharing [18].

The fidelity operator for that state $\hat{\mathcal{F}}_{\Psi_4}$ contains 40 relevant correlation operators ($\sigma_i \otimes \sigma_j \otimes \sigma_k \otimes \sigma_l$), out of which 21 describe four-qubit correlations (i.e. do not contain σ_0). Already 10 are enough to construct a characteristic Bell operator that has $|\Psi_4\rangle$ as non-degenerate

TABLE I: Maximal expectation values $\langle \hat{\mathcal{B}}_{\Psi_4} \rangle$

State	under LU	under SLOCC
$ \Psi_4\rangle$	1.000	1.000
$ D_4^{(2)}\rangle$	0.926	0.926
$ GHZ\rangle$	0.805	0.805
$ C\rangle$	0.515	0.764
$ W\rangle$	0.736	0.758
$ \text{bi-sep}\rangle$	0.722	0.749
$ \text{sep}\rangle$	0.217	0.217

TABLE II: Maximal expectation values $\langle \hat{\mathcal{B}}_{D_4^{(2)}} \rangle$

State	under LU	under SLOCC
$ D_4^{(2)}\rangle$	1.000	1.000
$ \Psi_4\rangle$	0.889	0.889
$ GHZ\rangle$	0.833	0.833
$ C\rangle$	0.500	0.706
$ \text{bi-sep}\rangle$	0.667	0.667
$ W\rangle$	0.613	0.619
$ \text{sep}\rangle$	0.178	0.178

eigenstate with maximum eigenvalue $\lambda_{\max} = 1$:

$$\begin{aligned} 6\hat{\mathcal{B}}_{\Psi_4} = & \sigma_x \otimes \sigma_y \otimes \sigma_y \otimes \sigma_x + \sigma_y \otimes \sigma_x \otimes \sigma_y \otimes \sigma_x \\ & - \sigma_y \otimes \sigma_y \otimes \sigma_x \otimes \sigma_x + \sigma_x \otimes \sigma_z \otimes \sigma_x \otimes \sigma_z \\ & + \sigma_z \otimes \sigma_x \otimes \sigma_x \otimes \sigma_z - \sigma_z \otimes \sigma_z \otimes \sigma_x \otimes \sigma_x \\ & + \sigma_z \otimes \sigma_z \otimes \sigma_z \otimes \sigma_z - \sigma_y \otimes \sigma_y \otimes \sigma_z \otimes \sigma_z \\ & + \sigma_y \otimes \sigma_z \otimes \sigma_y \otimes \sigma_z + \sigma_z \otimes \sigma_y \otimes \sigma_y \otimes \sigma_z. \quad (3) \end{aligned}$$

$\hat{\mathcal{B}}_{\Psi_4}$ can be used to discriminate an experimentally observed state with respect to other four-qubit states. With the chosen normalization we obtain the limit for any local realistic theory by replacing σ_i by some locally predetermined values $I_i = \pm 1$, leading to the inequality $|\langle \hat{\mathcal{B}}_{\Psi_4} \rangle_{\text{avg}}| \leq \frac{2}{3}$. Table I shows the bounds on the expectation value of $\hat{\mathcal{B}}_{\Psi_4}$ acting on some classes of prominent four-qubit states (including a fully separable state $|\text{sep}\rangle$, any bi-separable state $|\text{bi-sep}\rangle$, as well as the four-partite entangled Dicke state $D_4^{(2)}$ [19], the GHZ [20], W [2] and Cluster (C) [21] state). These bounds were obtained by numerical optimization over either LU- or SLOCC-transformations, respectively. In particular with the bound for an arbitrary bi-separable state $\hat{\mathcal{B}}_{\Psi_4}$ provides also a sufficient condition for genuine four-partite entanglement.

We now employ these results for the analysis of experimental data. To observe the state $|\Psi_4\rangle$ we used photons generated by type II non-collinear spontaneous parametric down conversion (SPDC) and a variable linear optics setup. Essentially, a four photon emission into two modes is overlapped on a polarizing beam splitter (PBS) and subsequently split into four modes. Depending on the setting of a half-wave plate (in our case oriented at 45°) preceding the PBS and conditioned on detecting a

photon in each of the four outputs, a variety of states can be observed [22]. The fidelity of the experimental state ρ_{Ψ_4} , determined from 21 four-qubit correlations, was $\mathcal{F}_{\Psi_4} = \text{Tr}[\hat{\mathcal{F}}_{\Psi_4}\rho_{\Psi_4}] = 0.90 \pm 0.01$. The analysis of the experimental state using the Bell operator $\hat{\mathcal{B}}_{\Psi_4}$ required less than half of the measurement settings and leads to $v_{\rho_{\Psi_4}} = 0.91 \pm 0.02$ (see Fig. 1a). This value is, according to Table I, sufficient to prove that the experimental state is genuine four-qubit entangled and cannot be of W-, Cluster-, or GHZ-type in the sense described above.

The class of states that can experimentally not be excluded as it has the second largest expectation value in Table I is represented by the so-called symmetric four qubit Dicke state [19, 23]

$$|D_4^{(2)}\rangle = \frac{1}{\sqrt{6}}(|0011\rangle + |0101\rangle + |0110\rangle + |1001\rangle + |1010\rangle + |1100\rangle). \quad (4)$$

In turn, for the Dicke state a separate, characteristic Bell operator $\hat{\mathcal{B}}_{D_4^{(2)}}$ can be constructed. Again, $|D_4^{(2)}\rangle$ has 40 correlation operators with non zero expectation value, out of which 21 describe original four-qubit correlations. Naturally, the exact values of the correlations T_{ijkl} differ compared to $|\Psi_4\rangle$. In the case of $|D_4^{(2)}\rangle$ they are such that eight of the correlation operators are already sufficient for the construction of $\hat{\mathcal{B}}_{D_4^{(2)}}$:

$$\begin{aligned} 6\hat{\mathcal{B}}_{D_4^{(2)}} = & -\sigma_x \otimes \sigma_z \otimes \sigma_z \otimes \sigma_x - \sigma_x \otimes \sigma_z \otimes \sigma_x \otimes \sigma_z \\ & -\sigma_x \otimes \sigma_x \otimes \sigma_z \otimes \sigma_z + \sigma_x \otimes \sigma_x \otimes \sigma_x \otimes \sigma_x \\ & -\sigma_y \otimes \sigma_z \otimes \sigma_z \otimes \sigma_y - \sigma_y \otimes \sigma_z \otimes \sigma_y \otimes \sigma_z \\ & -\sigma_y \otimes \sigma_y \otimes \sigma_z \otimes \sigma_z + \sigma_y \otimes \sigma_y \otimes \sigma_y \otimes \sigma_y \end{aligned} \quad (5)$$

with $\lambda_{\max} = 1$ for $|D_4^{(2)}\rangle$. This operator has a remarkable structure: It is of the form $\sigma_x \otimes M_3 + \sigma_y \otimes M'_3$, where M_3 and M'_3 are three-qubit Mermin inequality operators [7, 24]. Thus, by applying a kind of GHZ-argument [20], the bound for any local realistic theory can be determined to be $|\langle \hat{\mathcal{B}}_{D_4^{(2)}} \rangle_{\text{avg}}| \leq \frac{2}{3}$.

Table II shows the maximal expectation values of $\hat{\mathcal{B}}_{D_4^{(2)}}$ by the same set of four-qubit states as before. Considering the structure of $\hat{\mathcal{B}}_{D_4^{(2)}}$, further omitting correlation operators, for example one whole block $\sigma_x \otimes M_3$ (or $\sigma_y \otimes M'_3$), leaves us with a four-qubit Mermin-type Bell operator. The corresponding Bell inequality is still violated by $|D_4^{(2)}\rangle$. However, it is not characteristic anymore for $|D_4^{(2)}\rangle$ as it is maximally violated by the state $|GHZ\rangle_y = \frac{1}{\sqrt{2}}(|RRRR\rangle \pm |LLLL\rangle)$ and the biseparable state $|BS\rangle = \frac{1}{\sqrt{2}}(|+\rangle(|RRR\rangle \pm i|LLL\rangle))$ (where $|\pm\rangle = \frac{1}{\sqrt{2}}(|0\rangle \pm |1\rangle)$ and $|R, L\rangle = \frac{1}{\sqrt{2}}(|0\rangle \pm i|1\rangle)$ are the eigenstates of σ_x and σ_y , respectively). It is a particular property of the Dicke state to have correlations in two planes (x-z- and y-z-plane) of the Bloch sphere, whereas a GHZ state, for instance, is correlated only in

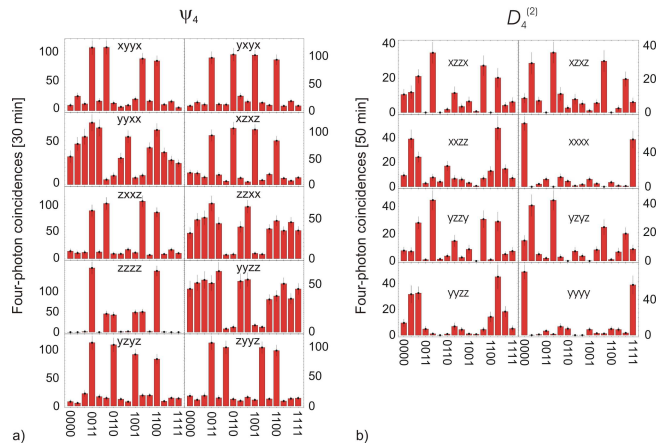


FIG. 1: Histogramms of the four-photon coincidence statistics for the different measurement settings. Slots at the ordinate indicate different events for a particular basis setting: e.g. 0011 for basis zzzz means detection of photons in the state $|HHVV\rangle$. a) Statistics of the ten correlation measurements, required for the evaluation of the operator $\hat{\mathcal{B}}_{\Psi_4}$. b) Statistics of the eight correlation measurements, required for the evaluation of the operator $\hat{\mathcal{B}}_{D_4^{(2)}}$.

one plane (here the x-z-plane). This quite characteristic feature is reflected in the construction of $\hat{\mathcal{B}}_{D_4^{(2)}}$. Recently, an experiment has been performed to observe the state $|D_4^{(2)}\rangle$ [23]. In order to increase the state fidelity \mathcal{F} by a higher degree of indistinguishability, here we reduced the filter bandwidth from 3 nm to 2 nm, resulting in $\mathcal{F} = 0.92 \pm 0.02$ (compared to $\mathcal{F} = 0.84 \pm 0.01$ in [23]). For the state's experimental analysis with the Bell operator (5) we find $v_{\rho_{D_4^{(2)}}} = 0.90 \pm 0.04$ (see Fig. 1b), from which we can conclude that it is genuine four-qubit entangled and cannot be, e.g., of W-, Cluster- or GHZ-type. Yet, this value is again just at the limit to separate against $|\Psi_4\rangle$.

If one is sure about the structure of the state space, that means that in our case it is spanned by four qubits, we can equally well use other operators instead of the Bell operators. Let us first drop some of the correlations from $\hat{\mathcal{B}}_{D_4^{(2)}}$, e.g., the terms $(\sigma_x \otimes \sigma_x \otimes \sigma_x \otimes \sigma_x)$ and $(\sigma_y \otimes \sigma_y \otimes \sigma_y \otimes \sigma_y)$. The resulting discrimination operator $\hat{\mathcal{D}}_{D_4^{(2)}}$ is not a Bell operator anymore, but still has $|D_4^{(2)}\rangle$ as the only eigenstate with maximal eigenvalue $\lambda_{\max} = 1$ (after proper normalization). Interestingly, as seen in Table III, it introduces a new ordering of states with a bigger separation between $|D_4^{(2)}\rangle$ and $|\Psi_4\rangle$. With $v_{\rho_{D_4^{(2)}}}^{\mathcal{D}} = 0.90 \pm 0.05$ we can discriminate against this state with a better significance. Note, the reordering, which results in the GHZ state having now the second highest eigenvalue, indicates that this operator analyzes the various states from a different point of view. This is quite plausible as it uses different correlations in the analysis. An even more radical change in

TABLE III: Alternative characteristic operators for $D_4^{(2)}$

State	$ \langle \hat{\mathcal{D}}_{D_4^{(2)}} \rangle $ (SLOCC)	$ \langle \hat{\mathcal{D}}'_{D_4^{(2)}} \rangle $ (SLOCC)
$ D_4^{(2)}\rangle$	1.000	1.000
$ GHZ\rangle$	0.905	0.937
$ C\rangle$	0.871	0.905
$ W\rangle$	0.869	0.905
$ \Psi_4\rangle$	0.869	0.901
$ \text{bi-sep}\rangle$	0.750	0.872
$ \text{sep}\rangle$	0.192	0.139

the point of view is possible with the data we dropped above, i.e., $(\sigma_x \otimes \sigma_x \otimes \sigma_x \otimes \sigma_x)$ and $(\sigma_y \otimes \sigma_y \otimes \sigma_y \otimes \sigma_y)$. Relying on the particular symmetries of the Dicke state, from these measurements we can evaluate the discrimination operator $\hat{\mathcal{D}}'_{D_4^{(2)}} = \frac{1}{6}((\frac{1}{2} \sum_k \sigma_x^k)^2 + (\frac{1}{2} \sum_k \sigma_y^k)^2)$, where e.g. $\sigma_{x/y}^3 = \mathbb{1} \otimes \mathbb{1} \otimes \sigma_{x/y} \otimes \mathbb{1}$ [25]. Comparing the observed value $v_{\rho_{D_4^{(2)}}}^{\mathcal{D}'_4} = 0.96 \pm 0.013$ with the bounds for other states (Table III) we see that we can discriminate our state against all states of the respective classes with only two settings. Analogous considerations can be applied for the construction of characteristic operators for other states [26], where the number of settings scales

polynomially with the number of qubits compared to the exponentially increasing effort for state tomography.

In conclusion, here we showed that characteristic (Bell-)operators, i.e., operators for which a particular state only has maximal expectation value, allow to distinguish this state from the ones out of other classes of multi-partite entangled states. A simple, though not yet constructive, method to design discrimination operators is based on the correlations between local measurement settings that are typical for the respective quantum state. The low number of measurement settings significantly diminishes the effort compared with standard analysis. Employing characteristic symmetries and properties of the state under investigation can even further reduce the effort to a number of settings which scales polynomially with the number of qubits, thereby rendering the new method a truly efficient tool for the characterization of multi-partite entanglement.

We thank D. Bruß, M. Horodecki, and M. Wolf for stimulating discussions. We acknowledge the support by the DFG-Cluster of Excellence MAP, the DAAD/MNiSW exchange program, the EU Projects QAP and SECOQC. W.W. is supported by QCCC of the ENB and the Studienstiftung des dt. Volkes, W.L. by FNP.

-
- [1] B. M. Terhal and P. Horodecki, Phys. Rev. A **61**, 040301(R) (2000); A. Sanpera, D. Bruß, and M. Lewenstein, Phys. Rev. A **63**, 050301(R) (2001); Y. Tokunaga, T. Yamamoto, M. Koashi, and N. Imoto, Phys. Rev. A **74**, 020301(R) (2006).
- [2] W. Dür, G. Vidal, and J. I. Cirac, Phys. Rev. A **62**, 062314 (2000).
- [3] F. Verstraete, J. Dehaene, B. DeMoor, and H. Verschelde, Phys. Rev. A **65**, 052112 (2002).
- [4] M. Horodecki, P. Horodecki, and R. Horodecki, Phys. Lett. A **223**, 1 (1996):
- [5] N. Gisin, Phys. Lett. A **154**, 201 (1991).
- [6] B.M. Terhal, Phys. Lett. A **271**, 319 (2000).
- [7] N. D. Mermin, Phys. Rev. Lett. **65**, 1838 (1990).
- [8] A. V. Belinskii and D. N. Klyshko, Phys. Usp. **36**, 653 (1993); W. Laskowski, T. Paterek, M. Żukowski, and C. Brukner, Phys. Rev. Lett. **93**, 200401 (2004); K. Nagata, W. Laskowski, M. Wieśniak, and M. Żukowski, Phys. Rev. Lett. **93**, 230403 (2004).
- [9] R. F. Werner and M. M. Wolf, Phys. Rev. A **64**, 032112 (2001); M. Żukowski and C. Brukner, Phys. Rev. Lett. **88**, 210401 (2002).
- [10] V. Scarani, A. Acin, E. Schenck, and M. Aspelmeyer, Phys. Rev. A **71**, 042325 (2005).
- [11] O. Gühne, G. Tóth, P. Hyllus, and H. J. Briegel, Phys. Rev. Lett. **95**, 120405 (2005); G. Tóth, O. Gühne, and H. J. Briegel, Phys. Rev. A **73**, 022303 (2006).
- [12] S. L. Braunstein, A. Mann, and M. Revzen, Phys. Rev. Lett. **68**, 3259 (1992); R. F. Werner, and M. M. Wolf, Phys. Rev. A **61**, 062102 (2000).
- [13] A. Acin, N. Gisin, and L. Masanes, Phys. Rev. Lett. **97**, 120405 (2006).
- [14] H. Weinfurter and M. Żukowski, Phys. Rev. A **64**, 010102(R) (2001).
- [15] M. Eibl, S. Gaertner, M. Bourennane, C. Kurtsiefer, M. Żukowski, and H. Weinfurter, Phys. Rev. Lett. **90**, 200403 (2003); S. Gaertner, M. Bourennane, M. Eibl, C. Kurtsiefer, and H. Weinfurter, Appl. Phys. B **77**, 803 (2003); J.-S. Xu, C.-F. Li, and G.-C. Guo, Phys. Rev. A **74**, 052311 (2006).
- [16] M. Bourennane, M. Eibl, S. Gaertner, C. Kurtsiefer, A. Cabello, and H. Weinfurter, Phys. Rev. Lett. **92**, 107901 (2004).
- [17] M. Murao, D. Jonathan, M. B. Plenio, and V. Vedral, Phys. Rev. A **59**, 156 (1999).
- [18] S. Gaertner, C. Kurtsiefer, M. Bourennane and H. Weinfurter, Phys. Rev. Lett. **98**, 020503 (2007).
- [19] R. H. Dicke, Phys. Rev. **93**, 99 (1954).
- [20] D. Greenberger, M. A. Horne, and A. Zeilinger, *Going beyond Bell's Theorem* (Kluwer Academic, Dordrecht, 1989); D. M. Greenberger, M. A. Horne, and A. Zeilinger, Am. J. Phys. **58**, 1131 (1990).
- [21] R. Raussendorf and H. J. Briegel, Phys. Rev. Lett. **86**, 5188 (2001).
- [22] W. Wieczorek et al., in preparation.
- [23] N. Kiesel, C. Schmid, G. Tóth, E. Solano, and H. Weinfurter, Phys. Rev. Lett. **98**, 063604 (2007).
- [24] The Bell inequality found by our method for the symmetric six-qubit Dicke state with three excitations, $|D_6^{(3)}\rangle$, is of the same structure: $\sigma_x \otimes M_5 + \sigma_y \otimes M'_5$. The bound for local realistic theories in this case is 0.4 and the expectation value for the Dicke state is 1 compared to e.g. 0.85

for any six-qubit GHZ state.

- [25] G. Tóth and O. Gühne, Phys. Rev. A **72**, 022340 (2005);
G. Tóth, J. Opt. Soc. Am. B **24**, 275 (2007).

- [26] G. Tóth and O. Gühne, Phys. Rev. Lett. **94**, 060501

(2005); O. Gühne, C.-Y. Lu, W.-B. Gao, and J.-W. Pan,
Phys. Rev. A **76**, 030305(R) (2007).

© 2008 The American Physical Society